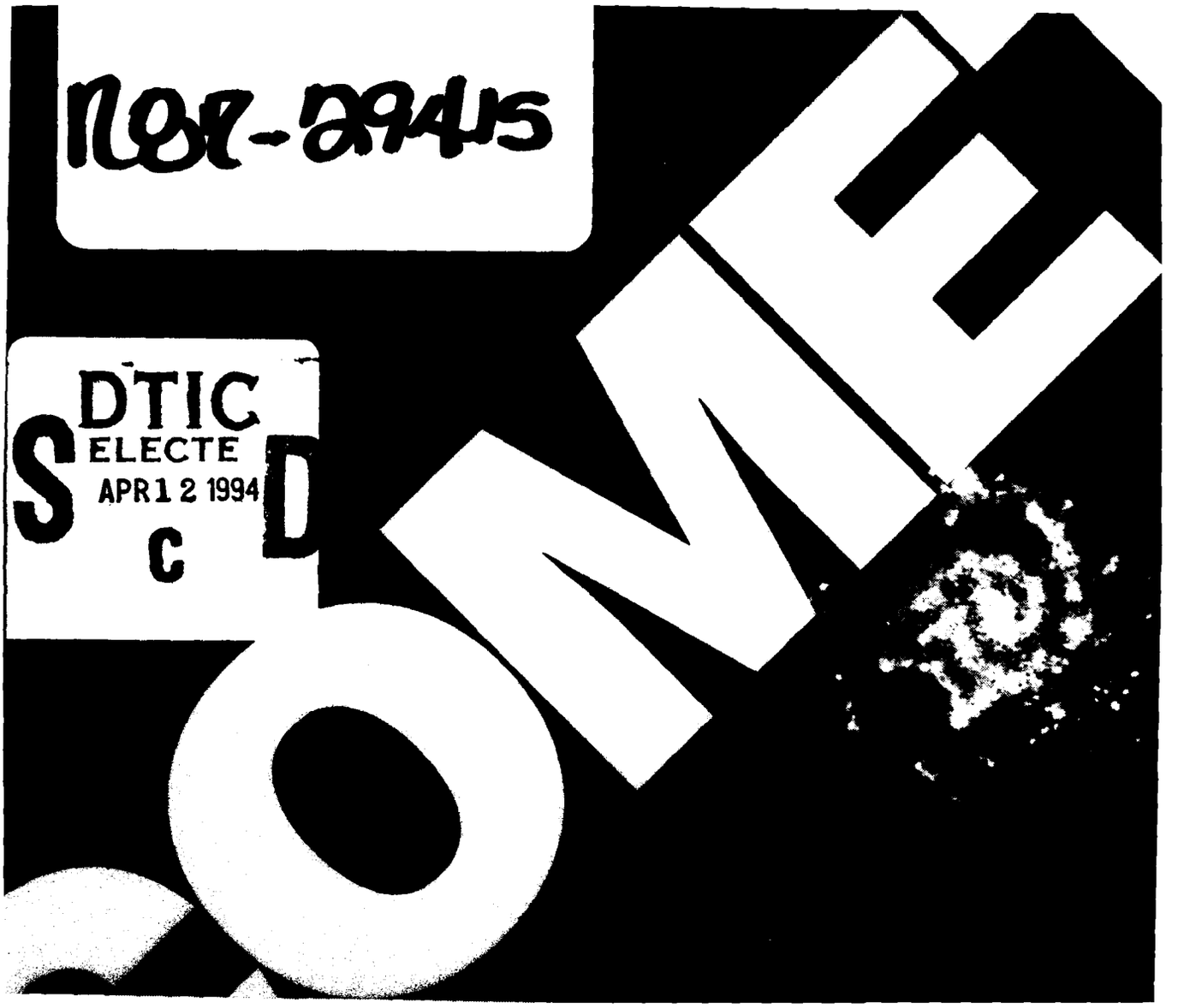
NSF-29415
DTIC
ELECTE
APR 12 1994
S
C
D
OME

The NASA STI Program ... in Profile

Since its founding, NASA has been dedicated to ensuring U.S. leadership in aeronautics and space science. The NASA Scientific and Technical Information (STI) Program plays an important part in helping NASA maintain its leadership role.

The NASA STI Program provides access to the NASA STI Database, the largest collection of aeronautical and space science STI in the world. The Program is also NASA's institutional mechanism for disseminating the results of its research and development activities.

A number of specialized services help round out the Program's diverse offerings, including creating custom thesauri, translating material to or from 34 foreign languages, building customized databases, organizing and publishing research results.

For more information about the NASA STI Program, you can:

- **Phone** the NASA Access Help Desk at (301) 621-0390
- **Fax** your question to NASA Access Help Desk at (301) 621-0134
- Send us your question via the **Internet** to help@sti.nasa.gov
- **Write to:**

  NASA Access Help Desk
  NASA Center for AeroSpace Information
  800 Elkridge Landing Road
  Linthicum Heights, MD 21090-2934

NASA CENTER FOR AEROSPACE INFORMATION

800 ELKRIDGE LANDING ROAD LINTHICUM HEIGHTS, MD 21090 (301) 621-0390

SHIPPED

MAR 30 199.

NASA Center for AeroSpace Information

ATTN: (PHONE)JOYCE
DATE OF REQUEST: 03/29/94
USER ID: 02672
ORDER CONTROL NUMBER: 940329100710
USER SECURITY LEVEL: SECRET RESTRICTED

ENCLOSED IS YOUR ORDER FOR 0001 HARDCOPY COPY **OF NASA ACCESSION NUMBER** N87-29415
TITLE: Parachute systems technology: Fundamentals, concepts, and applications.
REPORT NUMBER: DE87-011634

DOCUMENT CLASSIFICATION: UNCLASSIFIED
DISTRIBUTION LIMITATION STATEMENT: UNLIMITED 1

QUESTIONS CONCERNING THIS ORDER SHOULD BE DIRECTED TO DOCUMENT REQUEST SERVICES, NASA CASI, (301) 621-0390.
PLEASE INCLUDE YOUR ORDER CONTROL NUMBER WITH YOUR INQUIRY.

02672-940329100710
DEPT OF DEFENSE
DEFENSE TECHNICAL INFORMATION CENTER
ATTN: DTIC-OCP/JOYCE CHIRAS
CAMERON STATION BLDG 5
ALEXANDRIA VA 22304

02672-940329100710
DEPT OF DEFENSE
DEFENSE TECHNICAL INFORMATION CENTER
ATTN: DTIC-OCP/JOYCE CHIRAS
CAMERON STATION BLDG 5
ALEXANDRIA VA 22304

LEGIBILITY NOTICE

A major purpose of the Technical Information Center is to provide the broadest dissemination possible of information contained in DOE's Research and Development Reports to business, industry, the academic community, and federal, state and local governments.

Although portions of this report are not reproducible, it is being made available in microfiche to facilitate the availability of those parts of the document which are legible.

3

DISCLAIMER NOTICE

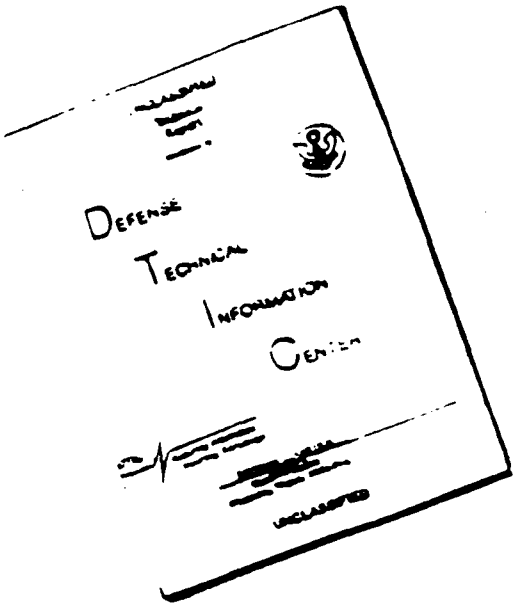

THIS DOCUMENT IS BEST QUALITY AVAILABLE. THE COPY FURNISHED TO DTIC CONTAINED A SIGNIFICANT NUMBER OF PAGES WHICH DO NOT REPRODUCE LEGIBLY.

CONF-870625--1

PARACHUTE SYSTEMS TECHNOLOGY: FUNDAMENTALS, CONCEPTS, AND APPLICATIONS

June 22-26, 1987

Munich, FRG

SAND--87-1648C

DE87 011634

Advanced Parachute Design*

Carl W. Peterson
Donald W. Johnson

Sandia National Laboratories
Albuquerque, New Mexico

Abstract

Advances in high-performance parachute systems and the technologies needed to design them are presented in this paper. New parachute design and performance prediction codes are being developed to assist the designer in meeting parachute system performance requirements after a minimum number of flight tests. The status of advanced design codes under development at Sandia National Laboratories is summarized. An integral part of parachute performance prediction is the rational use of existing test data. The development of a data base for parachute design has been initiated to illustrate the effects of inflated diameter, geometric porosity, reefing line length, suspension line length, number of gores, and number of ribbons on parachute drag. Examples of advancements in parachute materials are presented, and recent problems with Mil-Spec broadgoods are reviewed. Finally, recent parachute systems tested at Sandia are summarized to illustrate new uses of old parachutes, new parachute configurations, and underwater recovery of payloads.

* This work performed at Sandia National Laboratories supported by the U.S. Department of Energy under contract number DE-AC04-76DP00789.

Advanced Parachute Design

Carl W. Peterson
Donald W. Johnson

Sandia National Laboratories
Albuquerque, New Mexico

Introduction

A review of advances in parachute technology is contained in this paper. Technological advances in parachute design and performance are made possible by a variety of factors, including a better understanding of how parachutes work, new predictive tools such as computer design codes, advances in material technology, and new ideas in configuration and usage. New developments in each of these areas will be summarized.

Advances in Parachute Design and Performance Prediction Codes

The inflating parachute is among the most difficult aerodynamic systems to model. The oncoming flow is time dependent (because the parachute decelerates the payload) and asymmetric. Oncoming velocities can be supersonic, transonic, subsonic, or combinations of these speed ranges. The turbulent wake generated by the payload flows into the parachute causing a reduction in parachute drag and stability. The boundary conditions for the flow are determined by the parachute itself, yet its shape is determined by the pressures generated by the flow field. The flow field behind the canopy is separated, and air passes through the canopy for parachutes with geometric and/or material porosity. On some parachute systems, the air behind the canopy can catch up to the parachute/payload combination and cause the parachute to lose drag and collapse. Pressure distributions across the canopy are needed to define material strengths and stresses. Finally, the motion of the payload and parachute(s) relative to the ground must be calculated in order to estimate performance of the parachute system.

With such a formidable list of difficult aerodynamic problems that are fundamental to the operation of a parachute, it is not surprising that analytical or numerical modeling of parachutes was bypassed in favor of empirical design methods for many years. Modern computers have made it feasible to consider development of numerical models of parachute inflation. However, we are still limited in what can be modeled by our understanding of what should be modeled; bigger computers cannot be utilized properly until we achieve greater insight into the governing physical processes which control the inflation of a parachute. Purvis' paper on parachute dynamics modeling in these course notes (Ref. 1) describes the events on parachute inflation in greater detail and references approximate models of inflation, structural loads, and differential canopy pressure distribution which appear in the literature. A few recent additions to the parachute modeling literature are summarized below.

Sundberg has developed a new computer code to analyze the structure of radially symmetric parachutes. The new code is called CALA (for CAnopy Loads Analysis) and is a significant improvement in ease of use and in convergence compared to its predecessor, the CANO code (Refs. 2, 3). The finite element approach of CANO is used in CALA, but the equations have been reformatted and the method of solution has been changed, resulting in reliable convergence to physically meaningful solutions for all ribbon, solid, and ringslot-solid parachute canopies attempted to date. Details of the governing equations and their solution are given in Ref. 4. Figure 1 shows good agreement between CALA predictions of parachute shape and data obtained in a wind tunnel test of 3-ft-diameter parachutes (Refs. 5, 6). The CALA code is operational and has been used to design every new parachute system at Sandia since its development.

Strickland (Ref. 7), McCoy and Werme (Ref. 8), and Shirayama and Kuwahara (Ref. 9) are developing vortex methods for predicting parachute aerodynamics, including parachute drag, canopy pressure distributions, and the wake flow field behind the parachute. Steeves (Ref. 10) is attempting

to predict the same decelerator characteristics by solving the Navier-Stokes Equations. Recently, Strickland has made calculations of the two-dimensional incompressible flow around circular arcs, assuming potential flow and modeling the surface of the circular arc as a series of quadrilateral vortex panels. In addition to the vortex filaments which describe the surface of the arc, vortex panels are released into the wake behind the arc. The flow is started impulsively from rest with no wake vorticity. At subsequent times, vorticity is shed from separation points to form the wake behind the parachute, while the strength of the vortex filaments on the arc is changed to satisfy the normal velocity condition at each control point on the surface. The velocity approaching the arc can be a function of time, as is the case for a parachute.

Good agreement has been obtained between Strickland's calculations and an experiment by Sarpkaya for a 120-degree circular arc. The arc was subjected to the velocity history shown in Fig. 2 in Sarpkaya's water facility at the Naval Postgraduate School. Strickland made vortex panel calculations when the oncoming velocity was constant (Time "A" on Fig. 2) immediately after the oncoming flow began to decelerate (Time "B") and well after after flow deceleration was initiated (Time "C"). Figure 3 shows the calculated loci of vortex filaments in the wake of the 120-degree arc at each of these times; these calculations agree with flow visualization photographs taken by Sarpkaya. Calculated pressure coefficients on the base of the 120-degree arc (Fig. 4) show regions where the wake has recontacted the arc and is actually pushing it from behind. These calculations give hope that vortex panel methods may some day be able to predict the onset of parachute wake recontact and canopy collapse.

The advent of numerical models of parachute aerodynamics should not be construed as the last days of semi-empirical prediction techniques. Semi-empirical models are extremely useful as design tools because they require much less computer memory and execution time. The goal for developing semi-empirical parachute prediction techniques must be to find the right level of empiricism which allows a wide variety of parachutes to be modeled over a reasonable range of release conditions with acceptable accuracy without requiring the parachute designer to adjust empirical parameters in order to obtain valid results. In support of the continuing development of semi-empirical prediction codes at Sandia, Purvis is developing an extensive parachute data base using carefully controlled parachute models in a low speed wind tunnel. The purposes of his study are to use experimental data to identify the governing physical phenomena underlying parachute performance, as well as to format the data in a manner that extends its applicability. Reference 11 presents the first results of his experiments on the effects of inflated diameter, geometric porosity, reefing line length, and number of gores on the drag and radial force of solid and ribbons parachutes. This work is a first step in defining a complete data base for flat circular and conical ribbon parachutes.

Advanced Materials Development

For the last 40 years or so, the predominate material used in the fabrication of parachutes and most other decelerators has been nylon. Type 66 nylon, the fiber currently being produced for parachutes in the U.S., is required by the Military Specifications for both broadgoods and narrow tapes and webbings. Other fibers are also being produced that have application in the design of parachutes and recovery systems. This section will briefly describe some of the recent work at Sandia National Laboratories with parachute materials.

Nylon

Although a wide range of nylon tapes and webbings are available commercially and through the Mil-Specs, Sandia has designed some 2-inch-wide ribbons to meet program requirements for ribbon parachutes. Two that are currently being woven have reinforced selvage and a breaking strength of 1000 lbs and 550 lbs. Although there is a Mil-Spec 1000-lb ribbon, the porosity is very high and caused inflation problems in the development of a large parachute. The 550-lb ribbon fills a gap in the current Mil-Specs and is very efficient, weighing about 40% less than the Mil-Spec 460-lb flat ribbon. Sandia is also considering the development of a family of 2-inch-wide ribbons that are more resistant to shrinkage than the ribbons currently available in the U.S., but not much work has been completed as yet.

Recent requirements for large solid parachutes have required a serious look at nylon broadgoods, particularly materials with very low porosity. There are no Mil-Specs that describe these fabrics although the U.S. Forest Service has some specs for the parachutes used by the smoke jumpers. Our requirements are for materials with a porosity of about 5-20 $ft^3/ft^2/min$ and strengths of 90 lbs/in and 45 lbs/in. The desired weights are 2.0-2.2 and 1.0-1.1 oz/yd^2, respectively. Several different weaves will be investigated to develop the most efficient material that will meet the low porosity requirement with minimum calendaring. Specifications will be written to control all phases of production of the fabric including the fiber, the greige goods, and the finishing. In addition, the specs will require enough testing to insure the quality of the material.

One other current broadgoods requirement is for a material similar to the 1.1 oz/yd^2 Mil-C-7020 Type 1. We will also determine if there are more efficient weaves that will meet this requirement. The goal of this development program is to produce material that will meet the requirements with known high quality.

It should be mentioned that the U.S. parachute industry has been plagued with Mil-C-7020 Type 1 and 1A material that does not meet the specs. A condition first named "mystery warp" but now called "abraded warp" was present in a large quantity of material and caused a strength loss as high as 50%. The material was used to manufacture a large number of parachutes

which the government is refusing to accept. This has resulted in considerable litigation and also has increased the requirement for stringent acceptance inspection of the fabric. The present inspection is done visually, but there is a possibility the inspection can be accomplished by other means.

Kevlar

Most new materials development at Sandia in recent years has been in the Kevlar narrow fabrics. The narrow fabrics that are described in the current Mil-Spec were developed with fiber efficiency as the primary goal. As a result, it is nearly impossible to sew a joint that has reasonable (80-90%) efficiency in many of the materials. Several new designs have resulted from this problem in addition to the new designs to meet program requirements. The design of Kevlar narrow fabrics can be difficult, and considerable compromising is generally necessary to meet all of the requirements. A good, patient, developmental weaver is very helpful.

A discussion with Mr. Kostelezky in 1985 has led to a successful development program that is almost completed. On one of our designs, a 400-lb, 3/8-inch-wide Kevlar radial had to be joined to a braided, 400-lb Kevlar suspension line. The joint that was developed had an efficiency of about 80-85%, which was acceptable, but was very difficult to sew and inspect to insure the strength requirements would be met. Mr. Kostelezky was weaving nylon that was flat and transitioned to a round weave, thus eliminating the necessity for a sewn joint. A U.S. weaver, Bally Ribbon Mills, had also tried this method some time ago with nylon and was able to weave Kevlar with a transition from flat to round. Sandia Specifications are being written to describe this material, and production will start soon.

Sandia has not had any requirements for Kevlar broadgoods for use in a parachute drag surface, but 55-denier material has been successfully woven.

Other Materials

One other new material that is being investigated by some weavers is called Spectra 900 and Spectra 1000. The fiber is produced by the Allied Chemical Company and is polyethylene based. Some of the characteristics are shown in Fig. 5. This fiber has elongation similar to Kevlar but has very poor strength capability at elevated temperatures. However, the density is less than Kevlar. Tests conducted to date indicate acceptable joint efficiencies can be obtained with this material.

Conclusions

An extensive family of narrow fabrics is becoming available to the parachute designer both in nylon and Kevlar. Unfortunately, the situation in broadgoods is not as good, and the designer must exercise caution when using these materials.

A New Parachute Canopy Configuration

A new parachute configuration (Ref. 12) has been designed and tested in response to these stringent performance and weight requirements:

Payload weight - 3130 lbs
Rate-of-descent - 25 ft/sec at 5000-ft pressure altitude
Maximum load applied to payload - 20,000 lbs
Deployment velocity - 100 ft/sec to 300 KEAS
Deployment altitude - sea level to 18,600 ft
Maximum oscillations - 10 degrees from vertical
Pack weight - 120 lbs (90 lbs for the parachutes)
Pack volume - 2.9 ft^3

Due to the placement of the recovery parachute in the payload, every deployment will be crosswind. To meet the requirements at the 100 ft/sec deployment conditions, the parachute system must be fully inflated seven seconds after the start of deployment.

The 25 ft/sec terminal velocity requires a drag area of 5000 ft^2. Also the deployment velocity range means a variation in dynamic pressure between 10 lbs/ft^2 and 300 lbs/ft^2. These requirements preclude the use of a large single parachute system due to the long inflation at the minimum velocity condition. As a result, development of a clustered parachute system was pursued to meet these requirements.

Since the parachute system must be capable of deployment at a dynamic pressure of 300 lbs/ft^2 but have the highest possible drag coefficient, the parachute was designed as a 20° conical solid canopy with geometric porosity in the vent area to control the initial loading. The porosity is provided by 12-inch-wide rings, and the design is called a ringslot-solid canopy. After a literature search, it was conservatively estimated that a drag coefficient of 0.77 would be reasonable for this type of parachute. The basic design parameters for the canopy are as follows:

Constructed diameter	52.5 ft
Cone angle	20°
Number of gores	48
Number of rings	8
Width of rings	12 inch
Width of spaces	1 inch

The suspension lines are 60-ft-long and attach to a 10-ft-long dispersion bridle for an effective length of 70 ft.

Simultaneity of inflation and even distribution of the drag force is always a problem in a clustered parachute system. Based on tests conducted at Sandia National Laboratories with other clustered parachute systems using a new central reefing/disreefing system, a load distribution of 40%-40%-20% was thought to be achievable, at least during the periods of high loads. As a result, 8000 lbs was used as the design load for each parachute.

The parachute stress code CANO was used to determine the required strength of the materials for the parachute. Fullness was added to the dimensions of the rings starting with 10% fullness at the upper edge of ring 1 (vent) and decreasing linearly to zero at the lower edge of ring 8. The fullness significantly lowered the stresses in the ring material. The cloth used for rings 1-3 was 2.25 oz/yd^2 nylon and the material used for the remaining rings was 1.1 oz/yd^2 ripstop nylon. The rings are block construction. The solid part of the canopy is conventional bias construction using 1.1 oz/yd^2 nylon.

Since weight and volume are critical, the structure, with the exception of the nylon vent reinforcement and a similar reinforcement at the upper edge of the solid part of the canopy, are constructed from Kevlar materials. The radials are 500-lb Kevlar tape and the suspension lines are 400-lb braided Kevlar. The reefing ring retainers, pocket bands, and skirt reinforcement also are Kevlar.

To avoid exceeding the design load at 300 lbs/ft^2, the individual parachutes must be severely reefed to between 1.5% and 3% of full-open drag area during the first stage. Wind tunnel tests have indicated that, at such low reefing ratios, skin friction drag (with some "flag drag") is the largest contributor to the total drag. To minimize this contribution and increase the pressure drag contribution, the parachutes are reefed with both radial and mid-gore reefing rings.

The parachutes as fabricated weighed slightly less than 30 lbs.

Testing of this parachute system was divided into two phases. The first test series studied a single parachute with a vehicle weighing 1050 lbs to characterize the performance of the new canopy configuration by itself. After these single canopy tests were completed, the cluster of three parachutes were tested with a vehicle weighing 3300 lbs. All of the tests were conducted at the Sandia National Laboratories Test Range at Tonopah, Nevada, from an A7 aircraft. The test vehicles were instrumented to measure accelerations on three axes, and for the clustered parachute tests, the load developed by each parachute was measured by individual load cells. Two onboard cameras are used on each test vehicle. Cinetheodolites were operated and reduced to obtain trajectory data. Documentary coverage of parachute deployment, inflation, and stability was provided by tracking telescope cameras.

The tests with a single parachute were used to develop a reefing schedule that meets the system requirements and controls the loads to be within the structural capabilities of the parachute. Another important objective was to determine the drag coefficient for this type of parachute.

It became apparent after the first test that, at the very low first-stage reefing ratio, the canopy was not inflating properly and the drag was being produced by "flag drag." For the second test, the eight rings were coated with RTV silicone to reduce the porosity. The inflation of the canopy was much improved during this test. Subsequent parachutes were fabricated using a calendered, low porosity material for the rings. The tests also

indicated that two stages of reefing would be required to avoid overloading the parachute.

The cluster of three 52.5-ft-diameter parachutes was used on the next tests. For these tests, the parachutes were packed in an existing cylindrical deployment bag. The central reefing/disreefing system was used on all tests. The data from the first test indicated that the loads developed by the individual parachutes during the first stage were greater that the loads generated by the parachutes during the single parachute tests. The length of the first-stage reefing line was shortened to avoid overloading the canopy. Also, during this test series, the decision was made to use only radial reefing on the second stage in an attempt to increase the inflation rate when the parachutes are going to the second-stage and full-open condition.

Tests of other clustered parachute systems have shown that tethering the skirts of the parachutes together appears to offer some performance advantages. If one parachute lags the others during full inflation, the skirt of the slow canopy will be spread helping the inflation. Also, if the overrunning wake contacts the parachute system, the skirt tethers allow the wake to push the canopies aside without collapse and still control the relative position of the parachutes. Use of tethers with this parachute system has been difficult since there is very little structure near the skirt with sufficient strength to withstand the loads. Vent tethers have been used with more success since the canopy is stronger in that area and a vent parachute is required to control the position of the vent immediately after canopy stretch.

The flight tests have shown that the variable area vent cap does not work as intended due to failure of the material during the early stages of inflation. Weight and volume considerations prevent redesigning the vent cap to withstand the loads. The vent area of the parachute will be reduced by adding a ninth ring above the present upper ring and placing a lightweight, low porosity sacrificial vent cover on the outside of the vent lines.

Figure 6 shows the clustered parachute system during the first reefed stage, Fig. 7 shows the system during the second reefed stage, and Fig. 8 shows the parachute system fully inflated.

The normal reduction of the cinetheodolite data includes the calculation of the position of the test vehicle as a function of time. Using this position data, three components of velocity are determined. The two horizontal velocity components are then corrected for winds using the wind data measured for the test. Errors in the wind data can cause significant errors in the vehicle velocity data when the terminal velocity is low. An example is shown in Fig. 9. VA is the total vehicle velocity relative to the air, i.e., the two "corrected" horizontal velocities have been added vectorially with VZ. VZ is the vertical velocity component with no wind corrections since it was assumed that there is no vertical wind. After about 15 seconds, the test vehicle is in vertical terminal descent. If there was no wind at all during the test, the two velocities would be the same (the horizontal velocity is zero assuming a stable parachute system with no gliding). Since there is a considerable difference in the two velocities, it is

assumed that the wind data used in the data reduction is incorrect, even though the winds are measured as accurately as possible.

For these tests, the average vertical velocity was calculated by determining the altitude loss for a 10-second period when the vehicle is in terminal descent. The average density for this time is used to calculate the dynamic pressure. The total weight of the vehicle plus parachute (or parachutes) is used to determine the average drag area and then the drag coefficient. The parachute area is based on the constructed diameter. If the test data allowed, more than one 10-second period was used and included in the average.

Table 1 shows some of the data for the single parachute tests. As previously noted, there was no positive inflation during the second stage of the first test. The drag coefficients listed were calculated as described above. Since the parachute is slightly unstable, the high values are probably the result of the canopy gliding during the terminal descent.

Table 2 shows some of the data from the clustered parachute tests. The loads listed for each parachute for each stage are the maximum loads developed and do not necessarily occur at the same time. The loads measured by the load cells for one of the tests are shown in Figs. 10 and 11. Figure 10 shows the first-stage load in greater detail. The loads developed by the

Test No.	Deploy Dyn. Press. lbs/ft²	Max. First Stage Load lbs	Max. Second Stage Load lbs	Max. Full Open Load lbs	Avg. Terminal Drag Area ft²	Average Terminal C_D	Remarks
PTV1-1	110	3150	--	3360	2416	1.116	No positive second-stage inflation
PTV1-2	120	3990	2310	3045	2392	1.105	
PTV1-3	254	6930	3360	3255	2473	1.143	

Table 1. Results from Single Parachute Tests

Test No.	Deploy Dyn. Press. lbs/ft²	Max. First Stage Load lbs	Max. Second Stage Load lbs	Max. Full Open Load lbs	Avg. Terminal Drag Area ft²	Average Terminal C_D
PTV3-1	136	5300 5600 4700	4250 5000 2000	3200 5200 2700	5574	0.858
PTV3-2	141	3900 3400 3700	6000 6000 3300	6300 4300 3200	6401	0.986
PTV3-3	252	7000 6900 5600	3500 3000 3100	3300 5500 7000	6113	0.941

Table 2. Results from Clustered Parachute Tests

parachutes during the first stage are within the assumed 40%-40%-20% load distribution but, during the second and third stages, one parachute lags the other two and does not develop as much load as desired. The film data indicates that the lagging parachute is always the bottom parachute in the cluster. This parachute is always experiencing the lowest velocity due to the trajectory of the vehicle. A lagging parachute is acceptable from a programmatic standpoint as long as the other requirements are met and the structural capability of the parachutes is not exceeded.

The presently used 70-ft-diameter recovery parachute is packed in a nylon deployment bag built to fit an irregularly-shaped parachute compartment, as shown in Fig. 12. The density of the pack (about 40 lbs/ft^3) causes the pack to continually grow and change shape. As a result, the parachute must be either in a shipping container or in the crew module at all times. The clustered parachute system must conform to the irregular shape of the storage compartment, which has four flat sides, a flat bottom, and two flat planes on the top. Three parachutes have been packed in a four-panel bag manufactured from Kevlar with longitudinal lacing in the corners. This pack is shown in Fig. 13. Mechanical fixtures are necessary for production packing of the parachute system. The fixtures will assist the packing crews in lacing the bag panels and shaping the pack to the final required configuration. Experience with the prototype bag indicates that the Kevlar materials will enable the system to keep the shape without the use of a special container.

An Underwater Parachute System and Flotation Bag

A recovery system has been designed to recover and bring to the surface of the ocean a vehicle weighing 640 lbs under water and approximately 800 lbs in air. The vehicle has a terminal sink rate of 52-55 ft/sec. Data on the vehicle's hydrodynamic characteristics, including vehicle accelerations and angular rates, had to be recorded on board the test vehicle during water entry and the initial part of the underwater trajectory. To retrieve the data, the decision was made to attempt recovery of the complete vehicle which would also allow reuse of the vehicle for future testing. The recovery system includes a 4.2-ft-diameter ribbon parachute, a 13-ft^3 flotation bag, and a gas generator for inflating the bag. Reference 13 describes this system in greater detail. Results of the tests, along with a description of the recovery system, are summarized here.

Recovery System Requirements

A typical flight includes launch of the test payload by a single or two-stage solid rocket motor booster system followed by impact in the ocean at the desired test conditions. A timer is started at impact and approximately four seconds later the recovery system is deployed. The vehicle velocity is decreased by the drag of the parachute and the buoyant force developed by the flotation bag. The downward velocity is arrested and the vehicle returns to the surface. To maximize the time for data gathering without making the recovery system design unnecessarily difficult, the following requirements were established:

Vehicle weight in air	800 lbs
Vehicle weight in water	640 lbs
Maximum velocity at recovery	55 ft/sec
Typical recovery depth	400 ft
Maximum recovery depth	600 ft

Underwater Recovery System Design

The recovery system requirements indicated that the decelerator chosen must be capable of withstanding substantial loads since the dynamic pressure at deployment is approximately 3000 lbs/ft^2. For this application, a 20° conical ribbon parachute was selected. The parachute is 4.2 ft in constructed diameter, has 16 gores, and a suspension line length of 65 inches. Nine horizontal ribbons were spaced to give an unstrained geometric porosity of 10.7%.

The design of the flotation bag was not as straightforward as the design of the decelerator. To insure an adequate buoyancy margin, it was decided to use a flotation bag with a volume of 13 ft^3. Since the maximum water depth for recovery system operation was 600 ft, the pressure of the gas for inflating the bag would have to be greater than 270 lbs/in^2 to inflate the bag at that depth. If the gas source chosen could provide the gas required for those conditions, recovery at shallow depths would result in more gas than necessary to inflate the bag. For a closed bag, this would

require a pressure relief valve capable of handling large flow rates. Since the recovery system had to be pressure packed to fit in the vehicle, it was decided to use a flotation bag that was open on the lower end and let the excess gas flow out of that end. This would occur both during initial inflation of the bag and during the ascent phase of the recovery. A cylindrical bag with a maximum diameter of 18 inches and a hemispherical shape on the closed end was designed. With an open-ended bag, the maximum pressure the bag would experience results from the difference in depth of the upper and lower ends of the 98-inch-long bag (3.6 lbs/in^2).

The flotation bag is manufactured from polyurethane-coated nylon using ultrasonically bonded seams and is placed inside a bag made from Kevlar cloth and webbings. Since the bags are deployed at the maximum freestream dynamic pressure, the Kevlar bag protects the flotation bag during the initial deceleration phase of the recovery and also transmits the parachute loads into the vehicle. The source for the high pressure gas for the flotation bag is located in the test vehicle. The open end of the bag is attached inside the recovery system storage can in a manner than prevents the freestream water from entering the bag, but the excess gas can be vented when the vehicle has been slowed or has started to ascend. A schematic of the recovery system is shown in Fig. 14.

Several methods for storing the gas required for the flotation bag were considered during the initial stages of design of the test vehicle and recovery system. It soon became obvious that a stored gas system was not possible from a weight and volume standpoint. The system used in this program is a modification of the warm gas generator used to inflate the flotation bags on the MK-50 torpedo. The gas generator used on this recovery system has 2.8 lbs of ammonium nitrate propellant in a rubber-based binder that burns and combines with 14.5 lbs of carbon dioxide to produce gas at the pressures required for inflating the flotation bag. The gas generator system is supplied by the Rocket Research Company, Redmond, Washington.

Use of the gas generator introduced several problems that had to be considered in the design of the flotation bag system. The output temperature of the gas (600-700°F) required cooling before the gas contacted the polyurethane-coated nylon bag material. This was accomplished by flowing the gas through a Kevlar inflation tube coated with RTV silicone. The 4-ft-long tube also directs the gas toward the closed end of the flotation bag. In operation, the gas generator created a 2800 lbs/in^2 pressure wave that impacted and damaged the inflation tube when the burst disk operated. A steel diffuser was installed upstream of the inflation tube to attenuate the pressure wave. The average gas temperature in the bag when the gas generator is depleted is approximately 250°F. Since the water will cool the gas and consequently decrease the pressure and volume, a thermal analysis was conducted to insure the vehicle was rising and dumping excess gas before the gas cooled enough to cause a loss in volume. The analytic techniques used are described in Reference 14.

The recovery system is packed in a conventional deployment bag that is 12.25-inch diameter and 5-inch deep. Pressure packing is used to obtain pack densities approaching 38 lbs/ft^3. Deployment of the recovery system is

accomplished by ejecting the vehicle aft cover plate with three thrusters. Four-ft-long bridles are used to attach the plate to the deployment bag.

Underwater Recovery System Testing

Testing a recovery system with these requirements as a complete system is impossible other than in an actual flight; then acquisition of any data on system performance becomes very difficult and expensive. Tests were conducted on the components of the recovery system. The complete system was then tested by dropping it into a lake from a barge and allowing the test vehicle to reach terminal velocity before starting the deployment sequence. The tests conducted are described in this section.

There were several questions to be answered by the parachute testing: Will the parachute inflate, how much drag is generated, and can the recovery system be deployed from a conventional bag by ejecting the aft plate into the wake behind the vehicle. The tow basin at the David Taylor Naval Ship Research and Development Center, Bethesda, Maryland, was made available for a series of tests. Carriage V of the High Speed Hydrodynamic Basin was used for the tests. A parachute strut was attached to the carriage with a towing arm, a load cell, and the test vehicle, as shown in Fig. 15. The series of tests conducted included the body alone, the body with the aft cover attached to three bridles 4-ft long, the body with the uninflated flotation bag and the 4.2-ft-diameter parachute attached, and a deployment test of the recovery system without the gas generator.

The drag of the predeployed parachute behind the body is shown in Fig. 16. The drag produced by the body has been subtracted from the total drag value, but the data does include the drag of the uninflated flotation bag. The drag coefficient varies between 0.51 and 0.6 based on the 4.2-ft constructed diameter. The data from the runs with the body only and the body with the aft cover plate in tow is presented in Table 3 The drag coefficients are based on the 14.7-inch base diameter of the vehicle. The aft cover has a 5-inch-diameter hole in the center to equalize the pressure on both sides of the plate when the plate is attached to the vehicle. The tests indicated that the cover plate was quite stable in the wake behind the test vehicle.

Configuration	Vel. ft/sec	Total Drag (lbs)	Body Drag (lbs)	Plate Drag (lbs)	C_D (Body)	C_D (Plate)
Body	50.6	608	608	NA	0.2	NA
Body & Plate	42.2	2466	423	2043	0.2	0.97
Body & Plate	50.6	3467	608	2859	0.2	0.94

Table 3. Tow Basin Test Data

During the first entry in the tow basin, a deployment test was attempted, but a malfunction in the thrusters prevented the aft cover from separating from the vehicle. The recovery system was successfully deployed by a small guide surface pilot parachute thrown from the carriage moving at a velocity of 25 ft/sec. The peak load measured during the test was 8078 lbs with a steady state load between 4200 and 5050 lbs. A slow lateral oscillation of the parachute was noted.

After modifying the thrusters, another deployment test was attempted. For this test, the load cell was removed to avoid any damage that might occur due to overloading. The recovery system was successfully deployed by ejecting the aft cover with the three thrusters and using the drag of the cover to deploy the packed system. The velocity of the carriage was 42.2 ft/sec (dynamic pressure = 1783 lbs/ft^2) during the test run. Observers on the carriage, which weighs approximately 100,000 lbs, reported that there was no question when the parachute inflated since the carriage started to shake at that time.

Preliminary tests to verify the flotation bag structure were conducted in an open tank by attaching the Kevlar bag to the bottom of the tank and inflating the bag with air. Although the bag developed over 800 lbs of buoyant force, there was no damage to either the urethane-coated nylon bag or the Kevlar bag.

The warm gas generator was tested by the manufacturer as part of the normal development program. One generator was discharged into a closed chamber with extensive pressure and temperature instrumentation at a Sandia National Laboratories test facility. The results of this test indicated that the gas generator produced enough gas to meet the recovery system requirements.

The complete recovery system was tested at the David Taylor Naval Ship R&D Center, Acoustic Research Detachment, Bayview, Idaho (located on Lake Pend Oreille). The test vehicle with the recovery system was released from a barge and allowed to accelerate to the terminal velocity with a firing cable and safety line trailing. When the vehicle reached a depth of 400 ft, an electrical signal was sent to the vehicle to start the recovery sequence. The recovery system was deployed, and in approximately 60 seconds, the flotation bag returned to the surface of the lake. It appeared that the top of the bag rose about 5 ft above the surface, settled back to the surface, and then sunk slowly to the end of the safety line. The safety line was attached to a winch on the barge and the vehicle was brought back to the surface where it floated with about 18 inches of the flotation bag above the surface. The ascent velocity (estimated to be 10-12 ft/sec) caused the system to rise high enough above the equilibrium position to allow extra gas to vent from the open end of the bag. The downward momentum then caused the system to descend far enough below the new equilibrium position to start collapsing the lower end of the flotation bag and allowing it to sink. This scenario was later confirmed analytically.

The ribbon parachute, which was hanging to the side of the flotation bag, did not add enough drag to control the ascent velocity. To add

positive drag, a 4-ft-diameter guide surface parachute was attached to the flotation bag which only inflates during the ascent phase of the trajectory. The ascent velocity with the guide surface parachute is approximately 5 ft/sec. If the ascent velocity is too low, the cooling of the gas could cause loss of buoyancy before the system has ascended into lower pressure regions and starts venting gas. The test from the barge was repeated with a recovery system modified with a guide surface parachute and was completely successful.

A recent flight test of the recovery system was conducted from the Sandia National Laboratories Kauai Test Facility, Hawaii. The test vehicle entered the water at 2000 ft/sec with a flight path angle of 20 degrees. The recovery system was programmed to be deployed 4.5 seconds after an accelerometer sensed impact with the water, but the test vehicle never became buoyant and sunk in 3350 ft of water. The underwater tracking data, when it became valid about 10 seconds after water impact, indicated the velocity of the test vehicle to be approximately 8.5 ft/sec all the way to the bottom. This velocity had to be the result of the drag of the parachute. Subsequent recovery of the test vehicle and recovery system confirmed that the recovery system was deployed properly. A postmortem of the vehicle showed that problems with the electrical system had allowed only one thruster (out of three) to fire and eject the aft cover and prevented the gas generator from igniting.

References

1. Purvis, J. W. "Computer Simulation of Parachute Dynamics," presented at the Parachute Systems Technology: Fundamentals, Concepts and Applications Short Course, June 22-26, 1987, Munich, West Germany.

2. Mullins, W. M., Reynolds, D. T., Lindh, K. G., and Bottorff, M. R., "Investigation of Prediction Methods for the Loads and Stresses of Apollo Type Spacecraft Parachutes, Volume II - Stresses," NVR 6432, Northrop Corporation, Ventura Division, Newbury Park, CA, June 1970.

3. Muramoto, K. K. and Garrard, W. L., "A User's Manual for CANO 2," Sandia National Laboratories Contract No. 73-0540, University of Minnesota, Minneapolis, MN, January 1982.

4. Sundberg, W. D., "A New Solution Method for Steady-State Canopy Structural Loads," AIAA Paper No. 86-2489, AIAA 9th Aerodynamic Decelerator and Balloon Technology Conference, Albuquerque, NM, October 1986.

5. Pepper, W. B. and Reed, J. F., "Parametric Study of Parachute Pressure Distribution by Wind Tunnel Testing," AIAA Journal of Aircraft, Vol. 13, November 1976, pp. 895-900.

6. Heinrich, H. G. and Uotila, J. I., "Pressure and Profile Data of 20-Degree Conical Ribbon Parachutes (Volume I)," Sandia Laboratories Contract No. 02-4011, University of Minnesota, Minneapolis, MN, October 1976.

7. Strickland, J. H., "On the Utilization of Vortex Methods for Parachute Aerodynamic Predictions," AIAA Paper No. 86-2455, AIAA 9th Aerodynamic Decelerator and Balloon Technology Conference, Albuquerque, NM, October 1986.

8. McCoy, H. H. and Werme, T. D., "Axisymmetric Vortex Lattice Method Applied to Parachute Shapes," AIAA Paper No. 86-2456, AIAA 9th Aerodynamic Decelerator and Balloon Technology Conference, Albuquerque, NM, October 1986.

9. Shirayama, S. and Kuwahara, K., "Computation of Flow Past a Parachute by a Three-Dimensional Vortex Method," AIAA Paper No. 86-0350, AIAA 24th Aerospace Sciences Meeting, Reno, NV, January 1986.

10. Steeves, E. C., "Prediction of Decelerator Behavior Using Computational Fluid Dynamics," AIAA Paper No. 86-2457, AIAA 9th Aerodynamic Decelerator and Balloon Technology Conference, Albuquerque, NM, October 1986.

11. Purvis, J. W., "Parachute Drag and Radial Force," AIAA Paper No. 86-2461, AIAA 9th Aerodynamic Decelerator and Balloon Technology Conference, Albuquerque, NM, October 1986.

12. Johnson, D. W., "Status Report of a New Recovery Parachute System for the F111 Aircraft Crew Escape Module," AIAA Paper No. 86-2437, AIAA 9th Aerodynamic Decelerator and Balloon Technology Conference, Albuquerque, NM, October 1986.

13. Johnson, D. W., "A Recovery System for an Underwater Projectile," AIAA Paper No. 86-2466, AIAA 9th Aerodynamic Decelerator and Balloon Technology Conference, Albuquerque, NM, October 1986.

14. Kuntz, D. W., "Analyses of the ASP Test Vehicle Recovery System," Sandia National Laboratories Report SAND86-1916, April 1987.

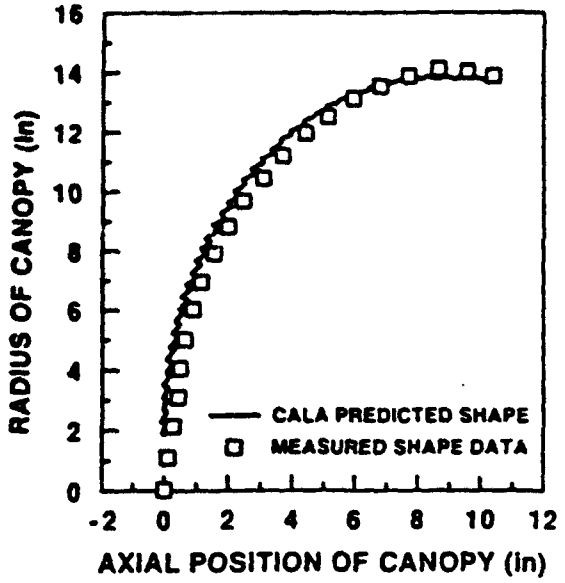

Figure 1: Canopy Loads Analysis (CALA) Parachute Shape Prediction

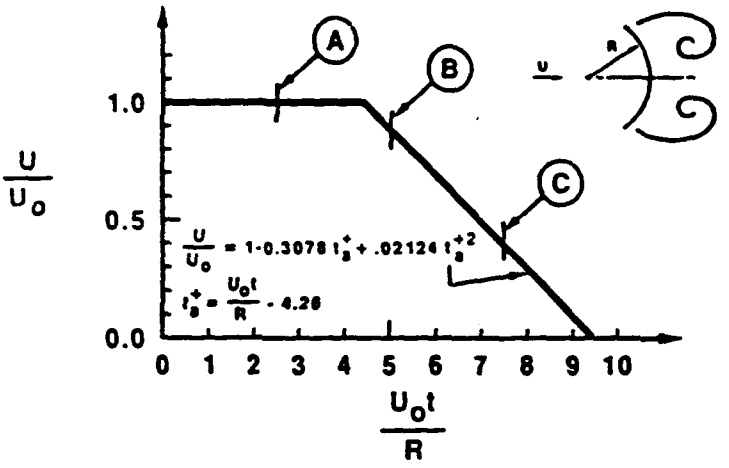

Figure 2: Velocity History for Flow Over a 120-Degree Circular Arc

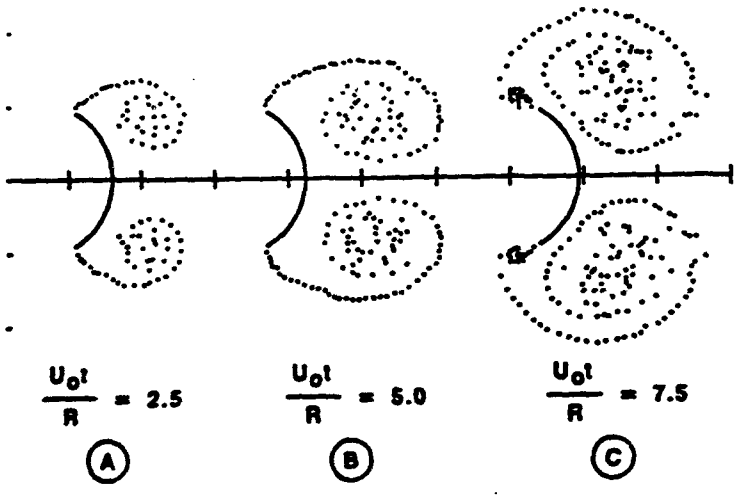

Figure 3: Vortex Panel Method Wake Geometry Calculations

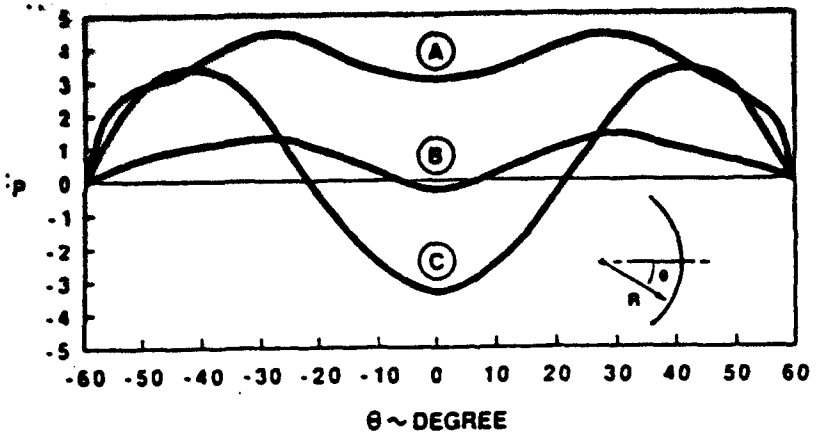

Figure 4: Vortex Panel Method Pressure Coefficient Calculations

Properties	SPECTRA® 900	SPECTRA® 1000	Aramid LM	Aramid HM	Graphite HS	Graphite HM
Strength (10^3 psi)	375	435	406	406	443	350
Elongation (%)	3.5	2.7	3.6	2.8	1.2	0.6
Tensile Modulus (10^6psi)	17	25	9.0	18.0	33	55
Specific strength (10^6in.)	10.7	12.4	7.8	7.8	6.8	5.4
Specific modulus (10^8in.)	486	714	173	346	507	846
Shrinkage at boil (%)	1	1	–	–	–	–
Specific gravity (lb./in.^{3})	0.035	0.035	0.052	0.052	0.065	0.065
Melting point (°C)	147	147	–	–	–	–
Filament size (microns)	38	27	12	12	7	7

	SPECTRA® 900	SPECTRA® 1000	Aramid LM	Aramid HM	Carbon HS	Carbon HM
Denier/No. filaments	[illegible]	[illegible]	[illegible]	[illegible]	[illegible]	[illegible]
Tenacity (g/denier)	30	36	22	22	20	14
Tensile modulus (gram)	1400	2000	450	970	1000	2400
Elongation (%)	3.5	2.7	3.6	2.8	1.2	0.6
Density (g/cc)	0.97	0.97	1.44	1.44	1.81	1.81

Figure 5: Material Characteristics Comparison

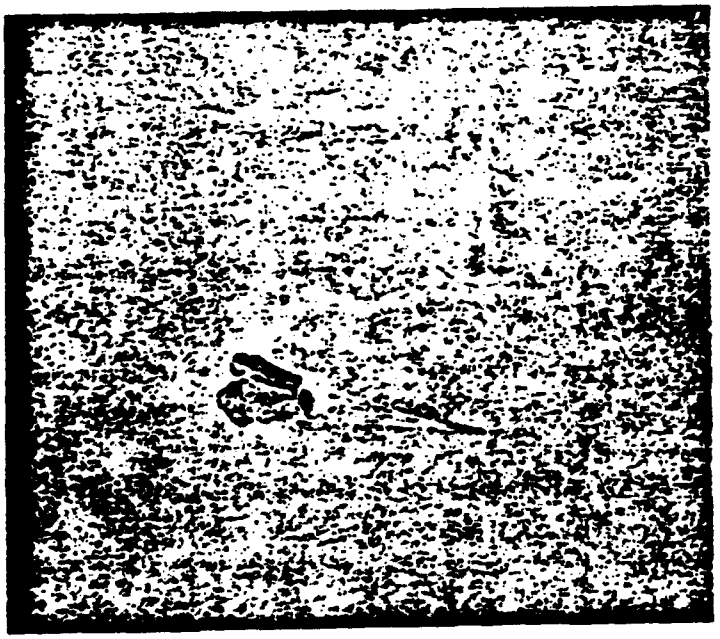

Figure 6: Clustered Parachute System, First Reefed Stage

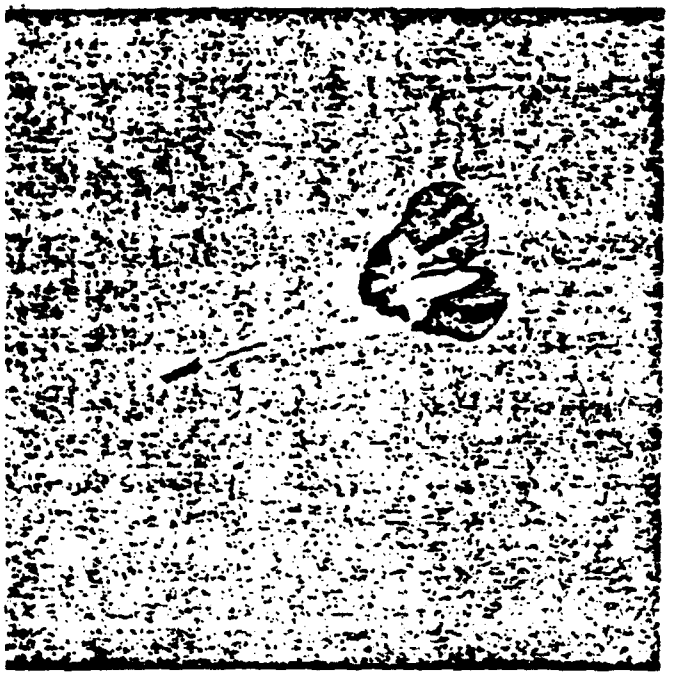

igure 7: Clustered Parachute System, Second Reefed Stage

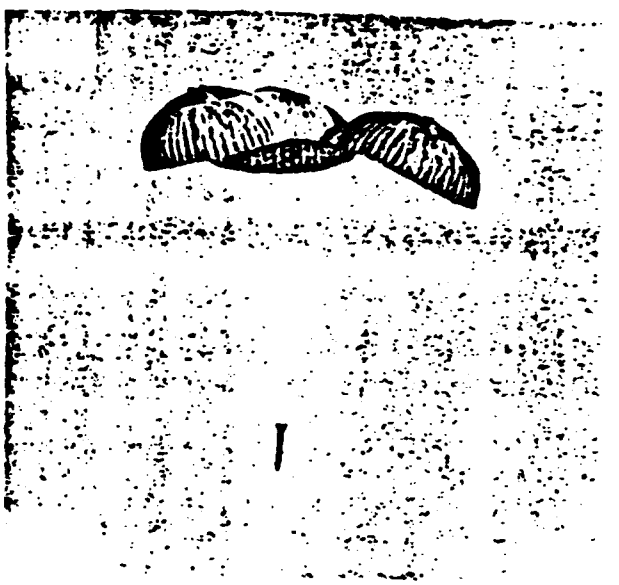

Figure 8: Clustered Parachute System in Terminal Descent

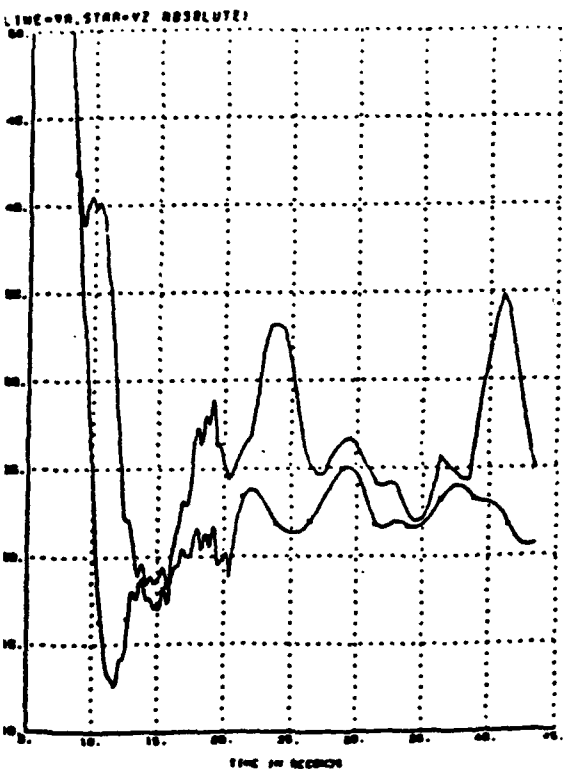

ure 9: Total Velocity and Vertical Velocity vs Time

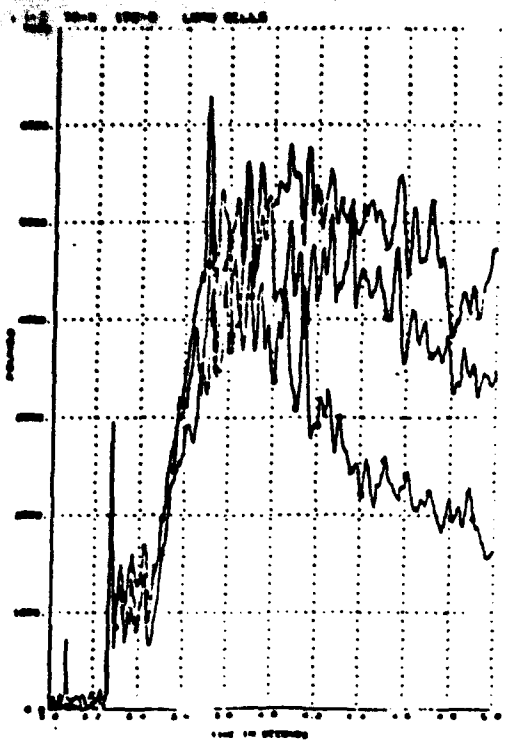

igure 10: Clustered Parachute Load Cell Data: First Stage Loads

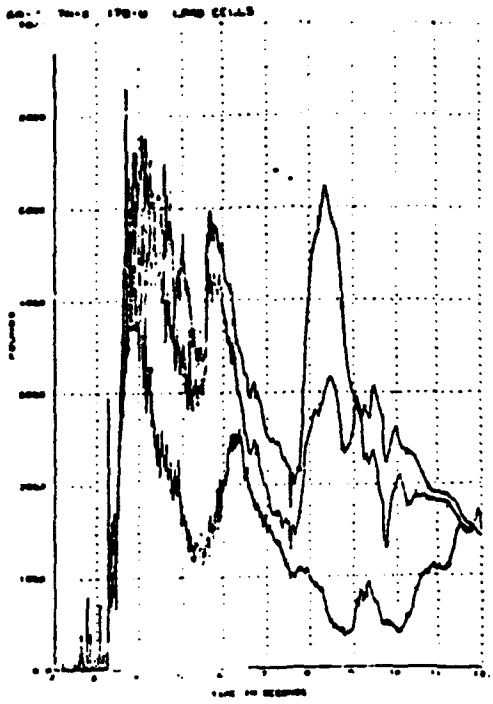

Figure 11: Clustered Parachute Load Cell Data for All Stages and Full-Open

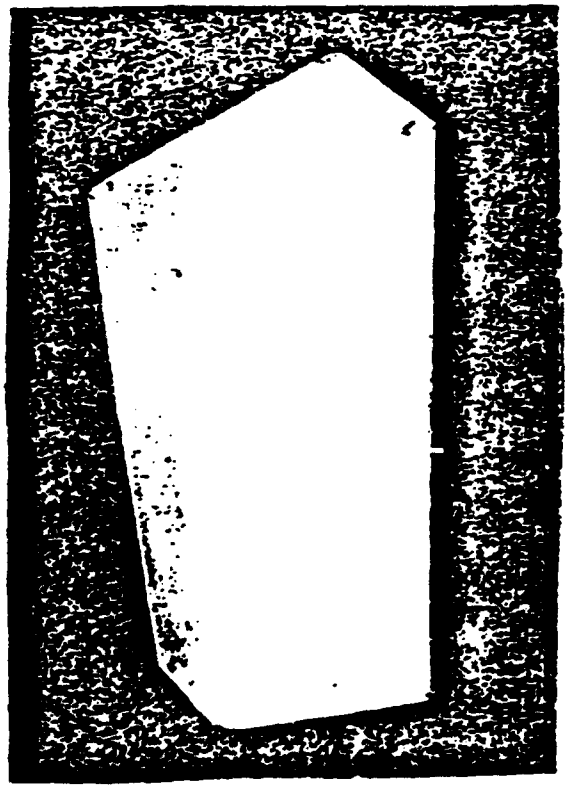

igure 12: Parachute Compartment Pattern

Figure 13: 52.5-ft-Diameter Parachute Cluster Packed in Kevlar Deployment Bag

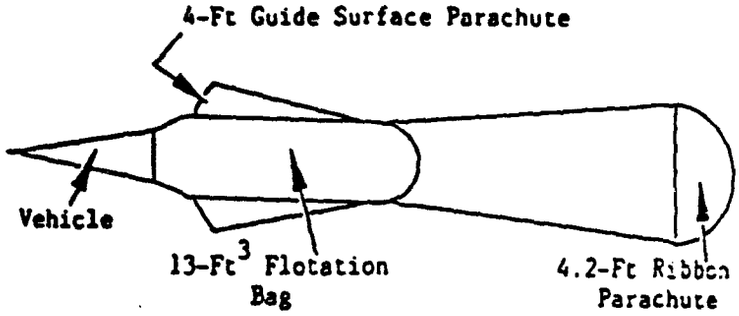

Figure 14: Underwater Vehicle Recovery System

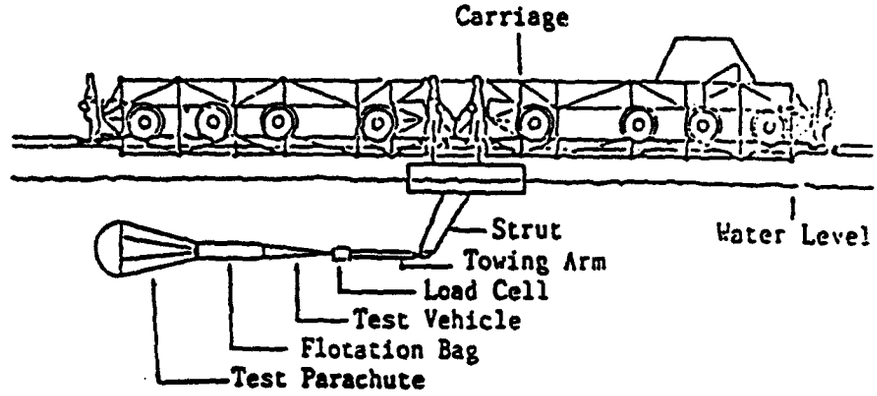

Figure 15: Towing Test Basin with Test Carriage

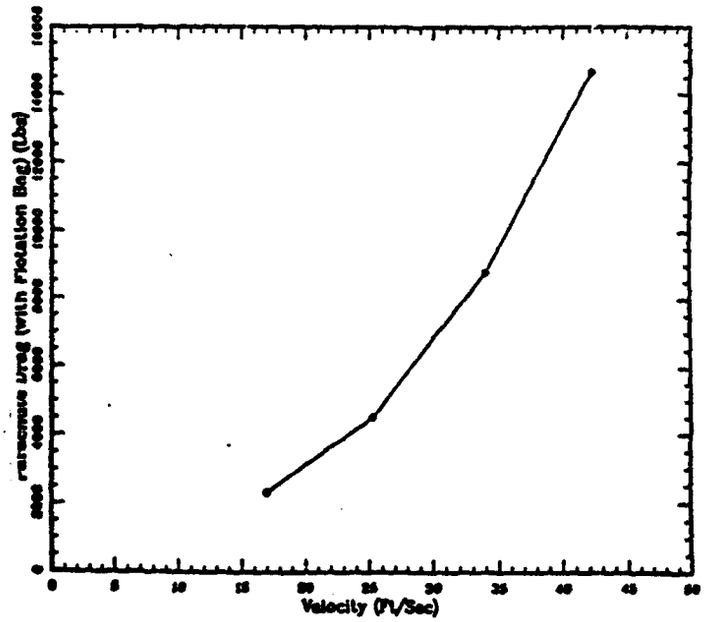

Figure 16: Underwater Parachute Drag (with Flotation Bag) Versus Velocity